

Dr. Armando
Romani

Computational neuroscience: biophysics - Lecture 5

Electrical Behavior of Neurons I

Lecture Overview

- Scope
- Approaches
- Applications

Lecture Overview

- Scope
- Approaches
- Applications

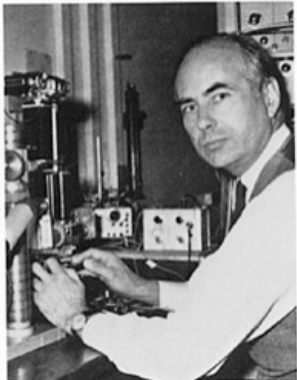
Hodgkin-Huxley (HH) model of the squid axon



Sir Alan Hodgkin, 1949

The Journal of Physiology, Vol. 263, No. 1

Frontispiece



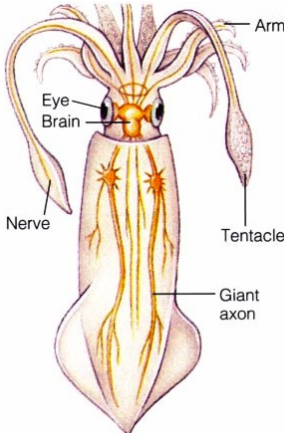
Sir Andrew Huxley, 1974



CHANCE AND DESIGN IN ELECTROPHYSIOLOGY:
AN INFORMAL ACCOUNT OF CERTAIN EXPERIMENTS
ON NERVE CARRIED OUT BETWEEN 1934 AND 1952

BY A. L. HODGKIN

From the Physiological Laboratory, University of Cambridge,
Downing Street, Cambridge CB2 3EG



1

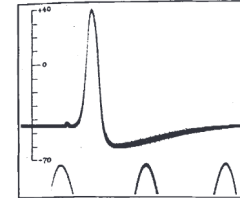
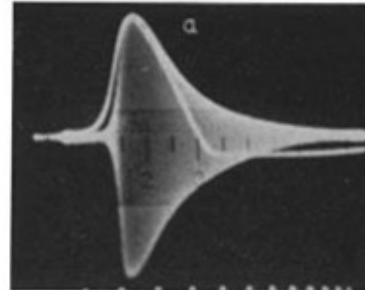


Fig. 2.

ACTION POTENTIAL RECORDED BETWEEN INSIDE AND OUTSIDE OF AXON. TIME MARKER, 500 CYCLES/SEC. THE VERTICAL SCALE INDICATES THE POTENTIAL OF THE INTERNAL ELECTRODE IN MILLIVOLTS, THE SEA WATER OUTSIDE BEING TAKEN AT ZERO POTENTIAL.

Cole KS, Curtis HJ. ELECTRIC IMPEDANCE OF THE SQUID GIANT AXON DURING ACTIVITY. *J Gen Physiol.* 1939

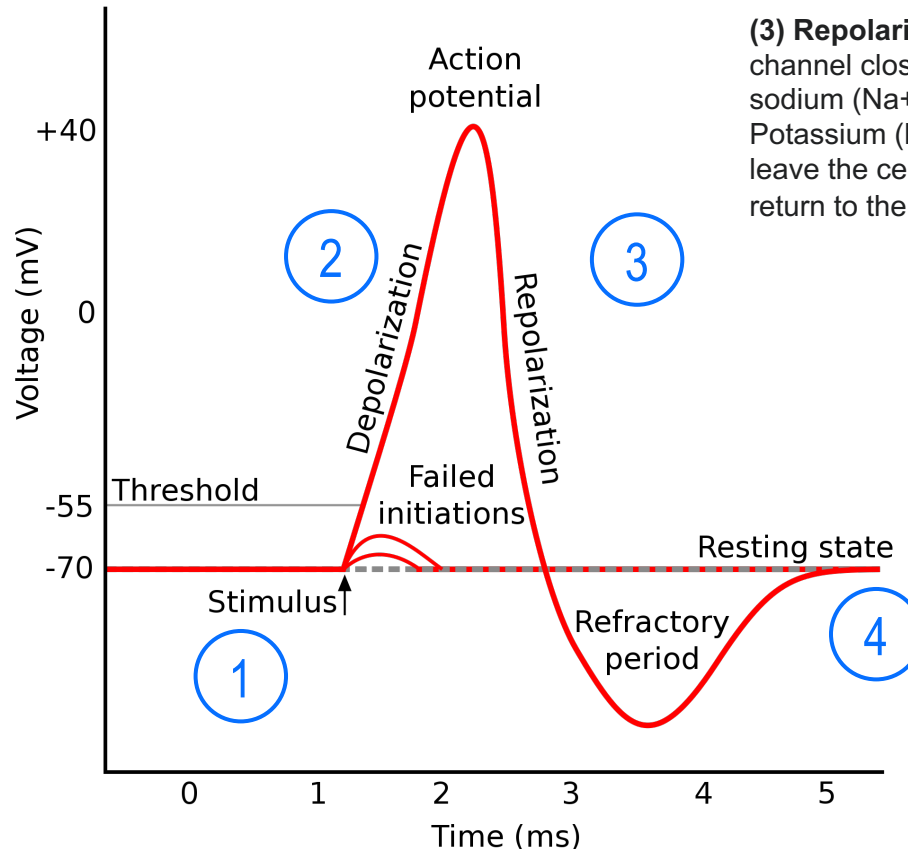
HODGKIN, A., HUXLEY, A. Action Potentials Recorded from Inside a Nerve Fibre. *Nature* 144, (1939)

Hodgkin AL & Huxley AF (1952) A Quantitative Description of Membrane Current and its Application to Conduction and Excitation in Nerve. *J Physiol* 117: 500–544.

Hodgkin-Huxley (HH) model of the squid axon

(1) Resting Potential: At rest, sodium (Na⁺) and potassium (K⁺) ions have limited ability to pass through the membrane, and the neuron has a net negative charge inside.

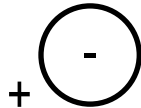
(2) Depolarization: With depolarization, sodium channels open and sodium (Na⁺) starts to enter the cell. Potassium channels open and potassium (K⁺) leaves the cell. Depending on the voltage, sodium dominates and leads to an action potential.



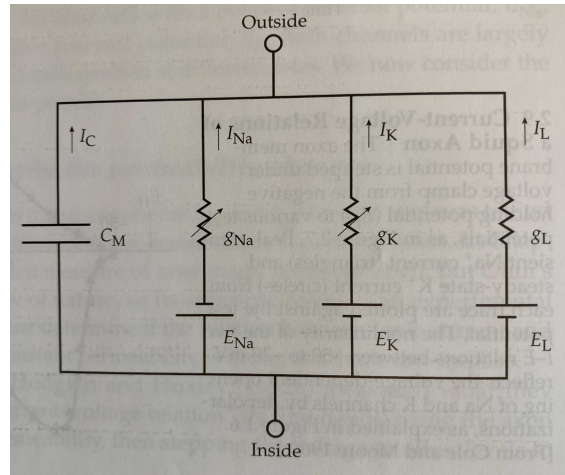
(3) Repolarization: Sodium channel close and no more sodium (Na⁺) enters the cell. Potassium (K⁺) continues to leave the cell, causing the return to the resting potential

(4) Resting Potential: Voltage-dependent ion channels are inactivated and Na⁺ and K⁺ concentrations return to their resting distribution

Hodgkin-Huxley (HH) model of the squid axon



$$V_m = V_i - V_e$$



A channel can be modelled as a resistance in series with a battery. If there is no difference in the concentration of the ions (e.g., K^+) between inside and outside, the current is due to the membrane voltage.

$$I_K = \gamma_K V_m$$

Where γ_K is the conductance for a single channel K^+

Hodgkin-Huxley (HH) model of the squid axon

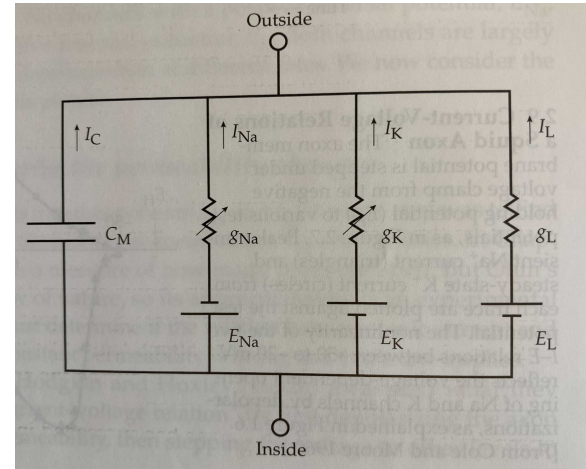
If there is a different in ion concentration, there is an electromotive force E_k given by the Nerst equation:

$$E_K = \frac{RT}{F} \ln \frac{[K]_o}{[K]_i} = 2.303 \frac{RT}{F} \log_{10} \frac{[K]_o}{[K]_i}$$

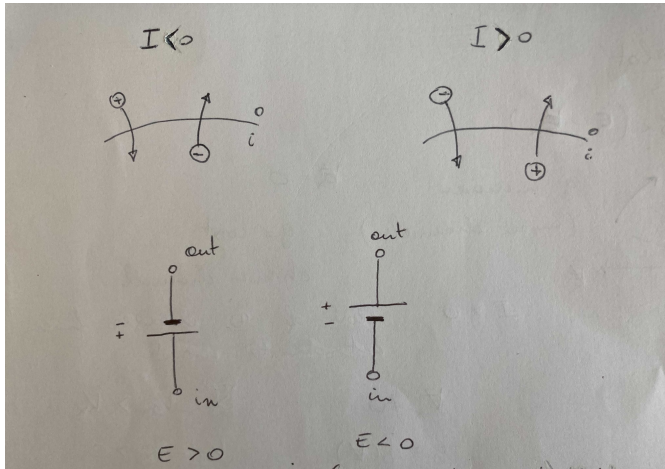
E_k is represented by a battery in the equivalent circuit.

The net driving force $V_m - E_k$

$$I_K = \gamma_K (V_m - E_k)$$



Hodgkin-Huxley (HH) model of the squid axon



$$E = E_i - E_e$$

TABLE 1.3 Free Ion Concentrations and Equilibrium Potentials for Mammalian Skeletal Muscle

Ion	Extracellular concentration (mM)	Intracellular concentration (mM)	$\frac{[Ion]_o}{[Ion]_i}$	Equilibrium potential ^a (mV)
Na ⁺	145	12	12	+67
K ⁺	4	155	0.026	-98
Ca ²⁺	1.5	100 nM	15,000	+129
Cl ⁻	123	4.2 ^b	29 ^b	-90 ^b

^aCalculated from Equation 1.11 at 37°C.

^bCalculated assuming a -90-mV resting potential for the muscle membrane and that Cl⁻ ions are at equilibrium at rest.

Hodgkin-Huxley (HH) model of the squid axon

In most of the cases, we have N channels and we can rewrite the expression with the total conductance g_K :

$$g_K = N_K \gamma_K$$

$$I_K = g_K(V_m - E_k)$$

Hodgkin-Huxley (HH) model of the squid axon

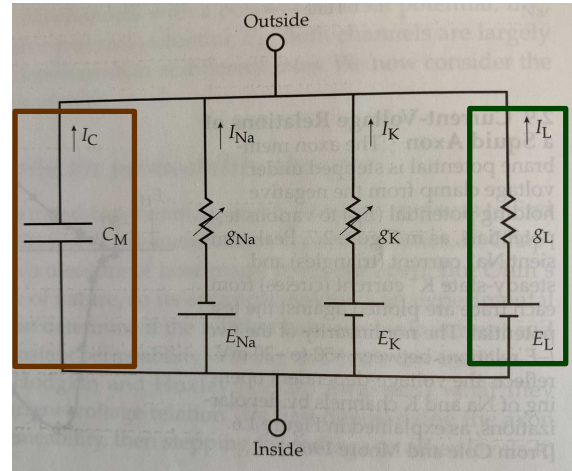
In a voltage-clamp experiment, the net current passing through the membrane I_M is split into a capacitive and ionic current:

$$I_M = I_C + I_i$$

$$I_i = I_K + I_{Na} + I_L$$

$$I_C = C_m \frac{dV_m}{dt}$$

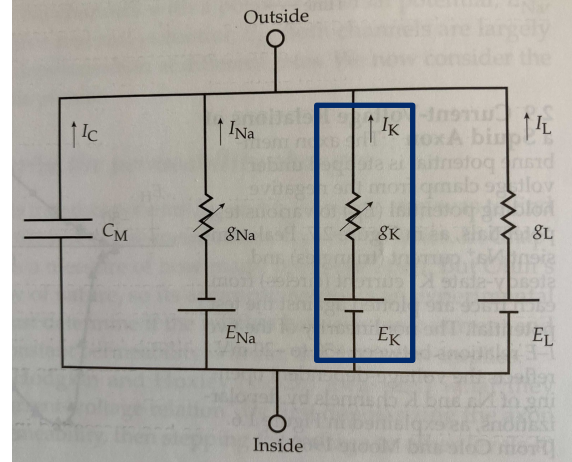
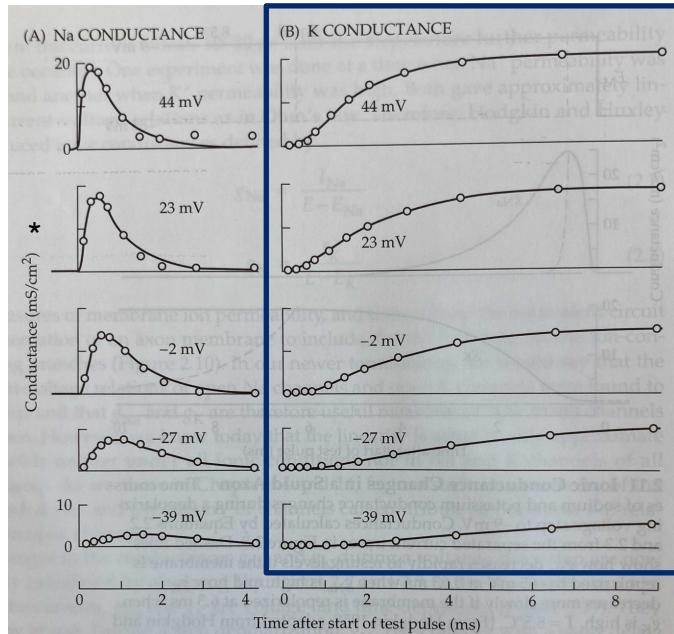
$$I_{leak} = g_{leak}(V_m - E_{leak})$$



Hodgkin-Huxley (HH) model of the squid axon

$$I_K = g_K(V_m - E_K)$$

g_K depends on time and voltage



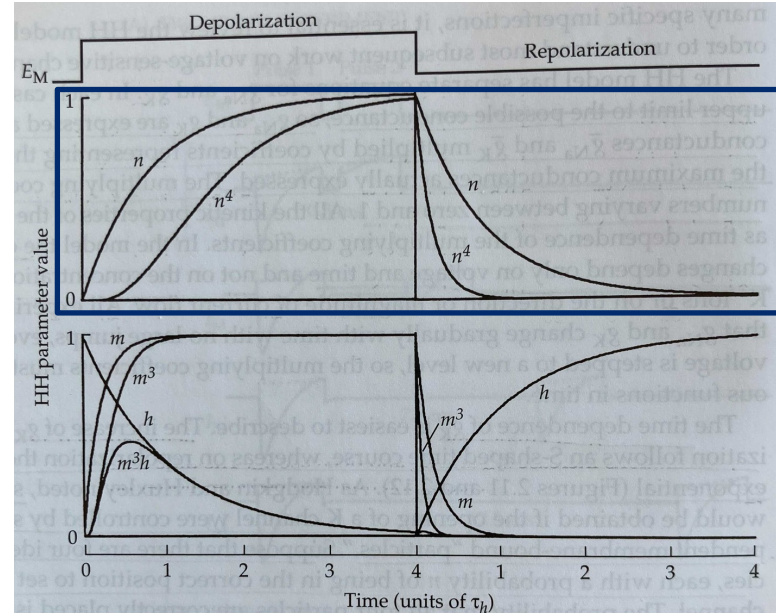
Hodgkin-Huxley (HH) model of the squid axon

$$I_K = g_K(V_m - E_K)$$

H.H. supposed that K channels are controlled by four independent “particles”. Each particle has a probability n to be in the correct position to open the channel (permissive). The probability that all the four particles are in the permissive state is n^4 .

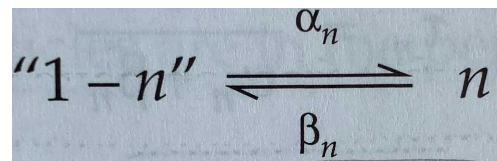
$$g_K = \bar{g}_K n^4$$

\bar{g}_K is the maximum conductance



Hodgkin-Huxley (HH) model of the squid axon

H.H. supposed that the particles are charged, so their distributions in the different states is voltage-dependent. Each particle moves between its permissive and nonpermissive state with first order kinetics. The rate constants are voltage-dependent and not time-dependent.

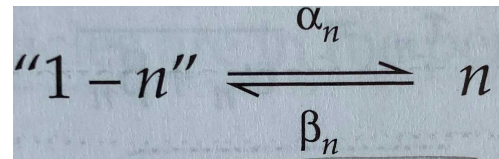


$$\alpha_n = 0.01 (V + 10) \left/ \left(\exp \frac{V + 10}{10} - 1 \right) \right.,$$

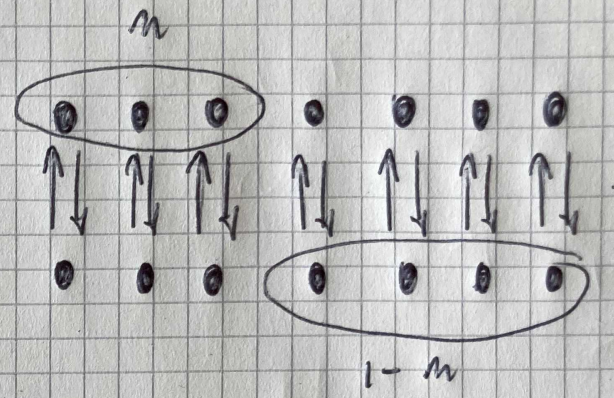
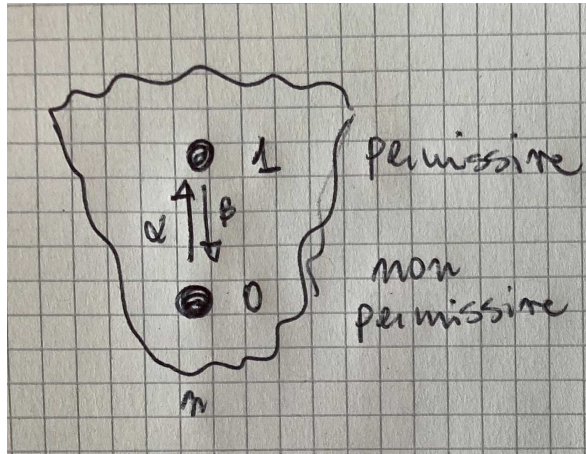
$$\beta_n = 0.125 \exp (V/80),$$

$$\frac{dn}{dt} = \alpha_n(1 - n) - \beta_n n$$

Hodgkin-Huxley (HH) model of the squid axon



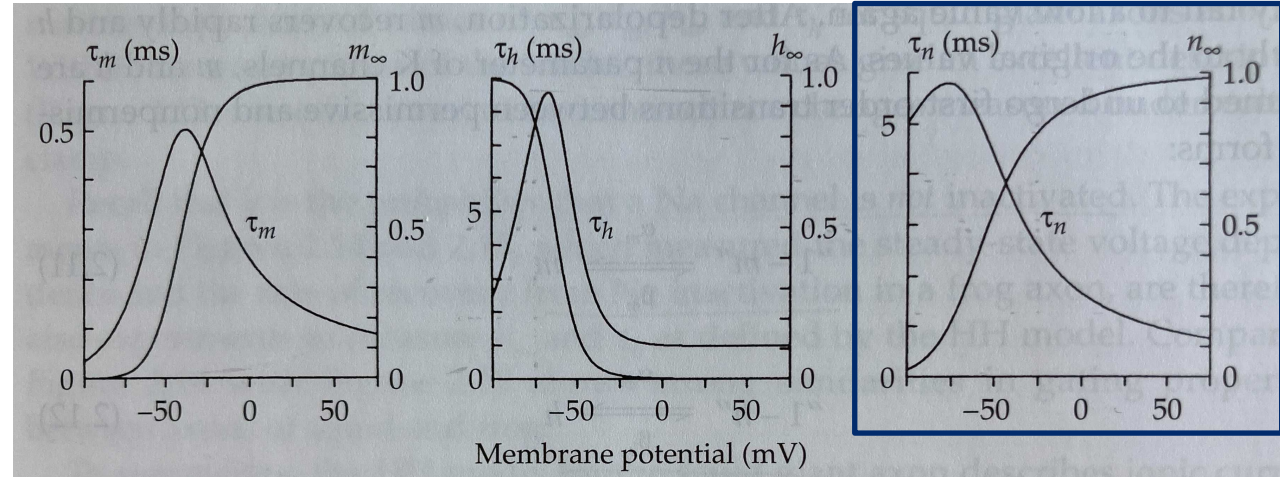
$$\frac{dn}{dt} = \alpha_n(1-n) - \beta_n n$$



Hodgkin-Huxley (HH) model of the squid axon

$$\tau_n = \frac{1}{\alpha_n + \beta_n}$$

$$n_\infty = \frac{\alpha_n}{\alpha_n + \beta_n}$$



$$\frac{dn}{dt} = \frac{n_\infty - n}{\tau_n}$$

$$n = n_\infty - (n_\infty - n_0) \exp(-t/\tau_n),$$

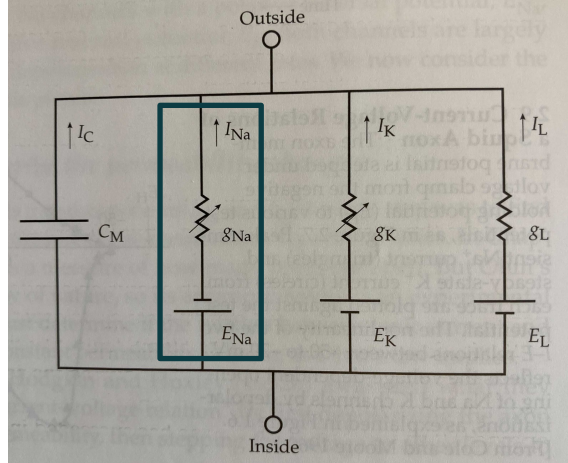
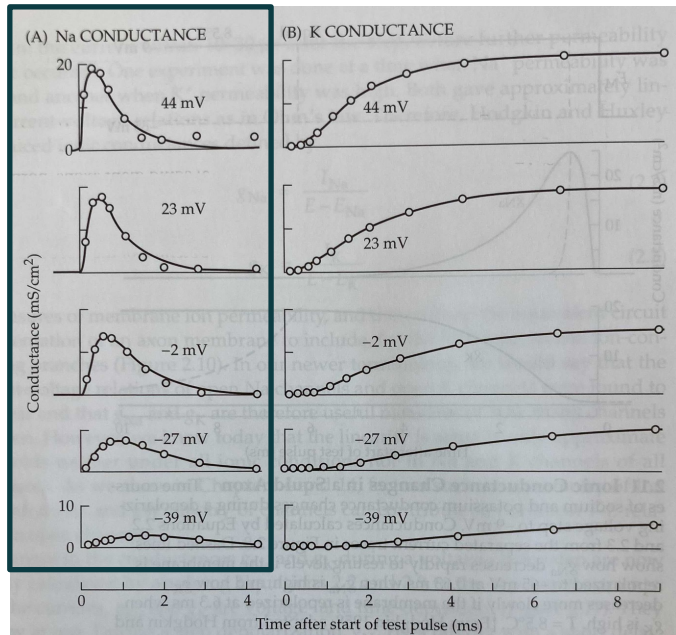
Hodgkin-Huxley (HH) model of the squid axon

- At resting membrane potential (RMP or V_m), beta \gg alpha, and particles n are in nonpermissive state. The conductance is zero, and the channel is closed.
- Following a depolarization, the rate constant alpha increases in a voltage-dependent manner, the distribution of particles changes and more particles n move into a permissive state. The change follows a first-order kinetics. The effect is the change of the conductance over time.

Hodgkin-Huxley (HH) model of the squid axon

$$I_{Na} = g_{Na} (V_m - E_{Na})$$

g_{Na} depends on time and voltage

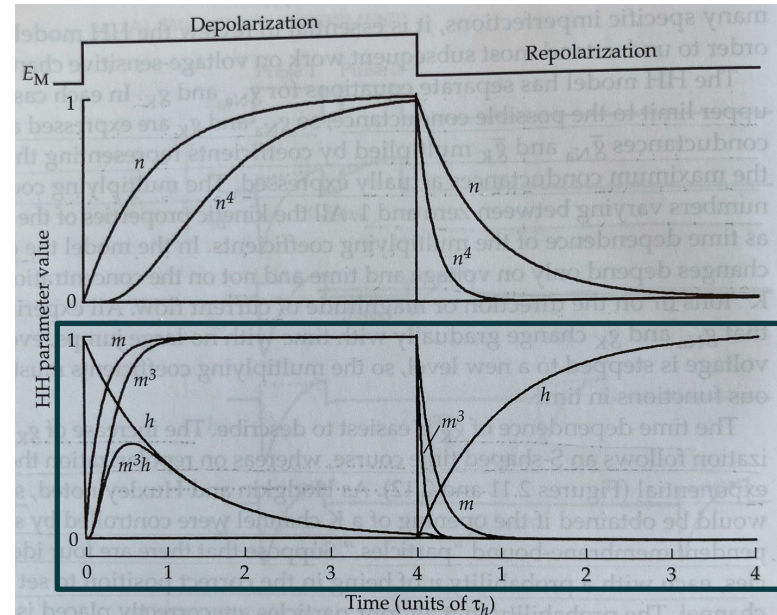


Hodgkin-Huxley (HH) model of the squid axon

$$I_{Na} = g_{Na}(V_m - E_{Na})$$

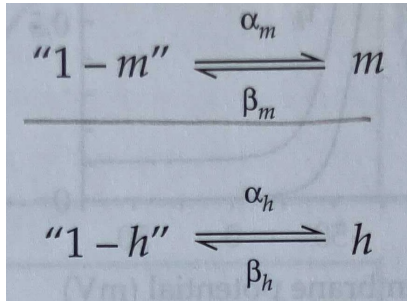
H.H. supposed that Na channels are controlled by two opposite gating processes: activation and inactivation. Activation is controlled by three m particles, while inactivation by one h particle. The probability that all the four particles are in the permissive state is m^3h (note that h is the probability that a Na channel is not inactive).

$$g_{Na} = \bar{g}_{Na}m^3h$$



Hodgkin-Huxley (HH) model of the squid axon

m and h are treated as n of the K channels



$$\frac{dm}{dt} = \alpha_m(1-m) - \beta_m m = \frac{m_\infty - m}{\tau_m}$$

$$\frac{dh}{dt} = \alpha_h(1-h) - \beta_h h = \frac{h_\infty - h}{\tau_h}$$

$$\begin{aligned} \alpha_m &= 0.1 (V + 25) \left/ \left(\exp \frac{V + 25}{10} - 1 \right) \right., \\ \beta_m &= 4 \exp (V/18), \\ \alpha_h &= 0.07 \exp (V/20), \\ \beta_h &= 1 \left/ \left(\exp \frac{V + 30}{10} + 1 \right) \right.. \end{aligned}$$

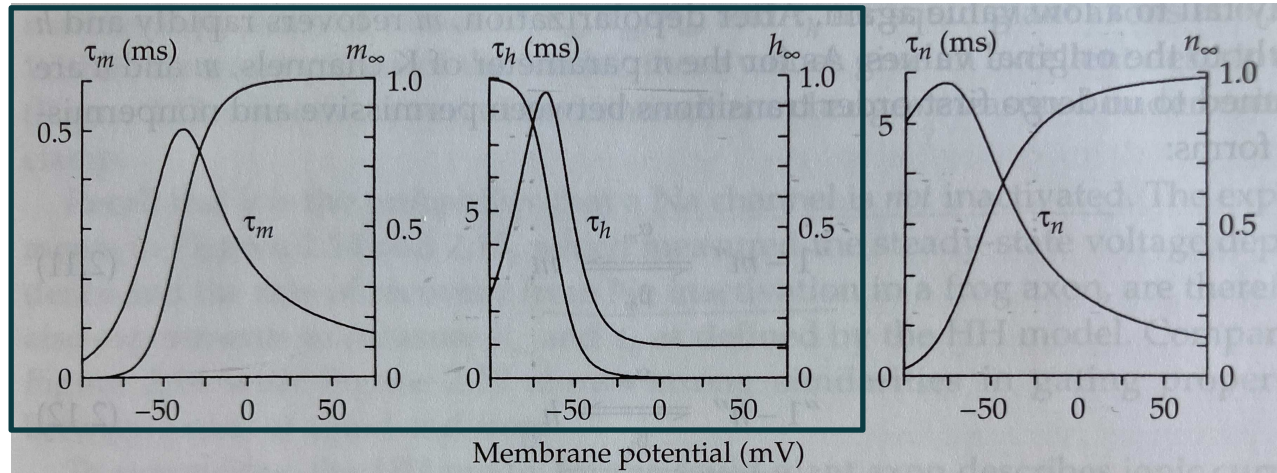
Hodgkin-Huxley (HH) model of the squid axon

$$\tau_m = \frac{1}{\alpha_m + \beta_m}$$

$$\tau_h = \frac{1}{\alpha_h + \beta_h}$$

$$m_\infty = \frac{\alpha_m}{\alpha_m + \beta_m}$$

$$h_\infty = \frac{\alpha_h}{\alpha_h + \beta_h}$$



$$m = m_\infty - (m_\infty - m_0) \exp(-t/\tau_m),$$

$$h = h_\infty - (h_\infty - h_0) \exp(-t/\tau_h),$$

Summary 1

- Hodgkin and Huxley modelled the generation of action potential in the axon of the giant squid and not in the neuron.
- HH model can be used for simplified neuron models (one compartment), where we are mainly interested in the generation of action potentials.
- Hodgkin and Huxley considered generic Na and K channels. We now know that there is a family of Na and K channels with different properties (see lecture 4).
- They considered not single channels but “populations” of channels (note that conductance is expressed as mS/cm^2)

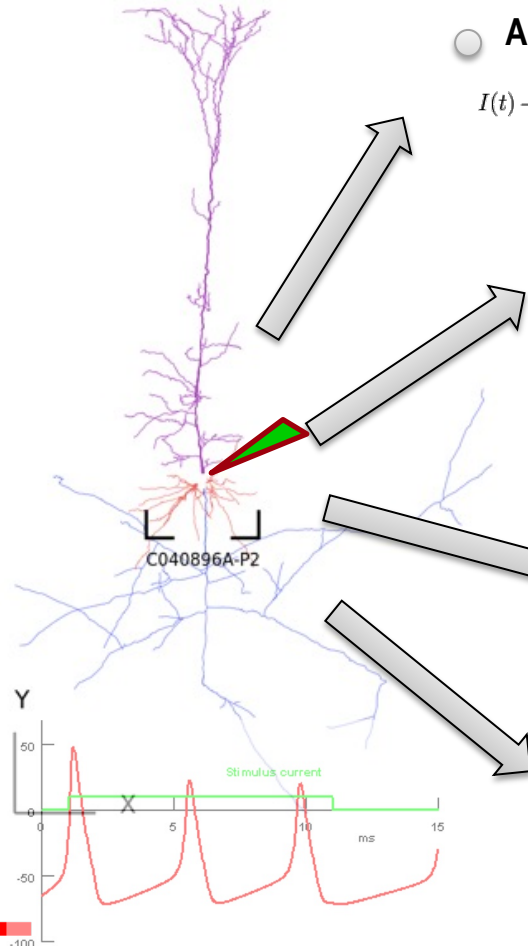
Summary 1

- The HH model fails to capture the role of the different compartments of the neuron (mainly the dendrites) (see below the example of Mainen et Sejnowski, 1996) and the variety of the ion channels present in the neurons with their specific properties and distributions which shape electrical properties of each cell. This is the subject of the current and next lectures.
- Even though HH model considers only Na and K currents, the HH formalism can be used for other types of channels.

Lecture Overview

- Scope
- **Approaches**
- Applications

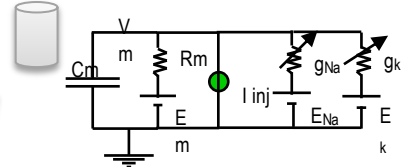
Many Ways to Modeling a Neuron



Abstract Model: Point neuron, e.g. Leaky Integrate and Fire

$$I(t) - \frac{V_m(t)}{R_m} = C_m \frac{dV_m(t)}{dt} \quad f(I) = \begin{cases} 0, & I \leq I_{th} \\ [t_{ref} - R_m C_m \log(1 - \frac{V_{th}}{I R_m})]^{-1}, & I > I_{th} \end{cases}$$

Simplified Model: Single Compartment and ion channel formalism



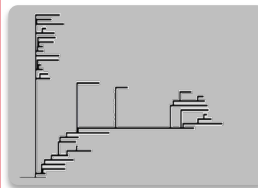
$$\frac{C_m dV_m}{dt} = \frac{E_m - V_m}{R_m} + I_{channels}$$

$$\frac{dm}{dt} = \alpha_m(V_m)(1 - m) - \beta_m(V_m)m$$

$$\frac{dh}{dt} = \alpha_h(V_m)(1 - h) - \beta_h(V_m)h$$

$$I_{channel} = m^n h g_{channel}(V_m - E_{channel})$$

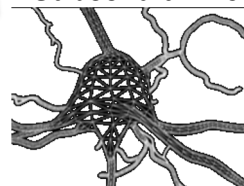
Cellular Model: Cable and ion channel formalism



$$\frac{C_m dV_m}{dt} = \frac{E_m - V_m}{R_m} + I_{channels}$$

$$+ \frac{2(V_{m_{i+1}} - V_{m_i})}{R_{a_{i+1}} + R_a} + \frac{2(V_{m_{i-1}} - V_{m_i})}{R_{a_{i-1}} + R_a}$$

Subcellular Model: Reaction-Diffusion formalism



$$\dot{p}(\mathbf{x}; t) = -p(\mathbf{x}; t) \sum_{\mu=1}^M a_{\mu}(\mathbf{x}) +$$

$$\sum_{\mu=1}^M p(\mathbf{x} - \mathbf{s}_{\mu}; t) a_{\mu}(\mathbf{x} - \mathbf{s}_{\mu})$$

Cable Theory of the Dendrites

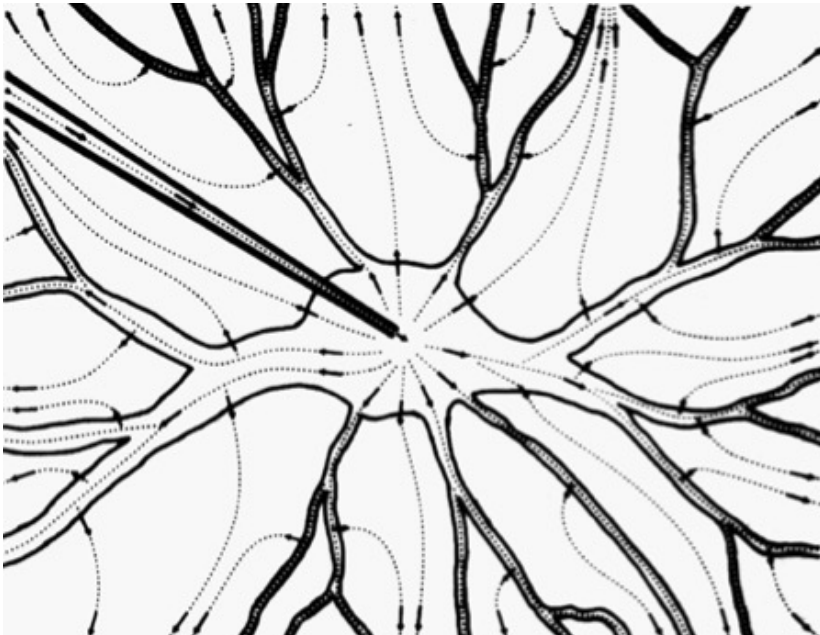


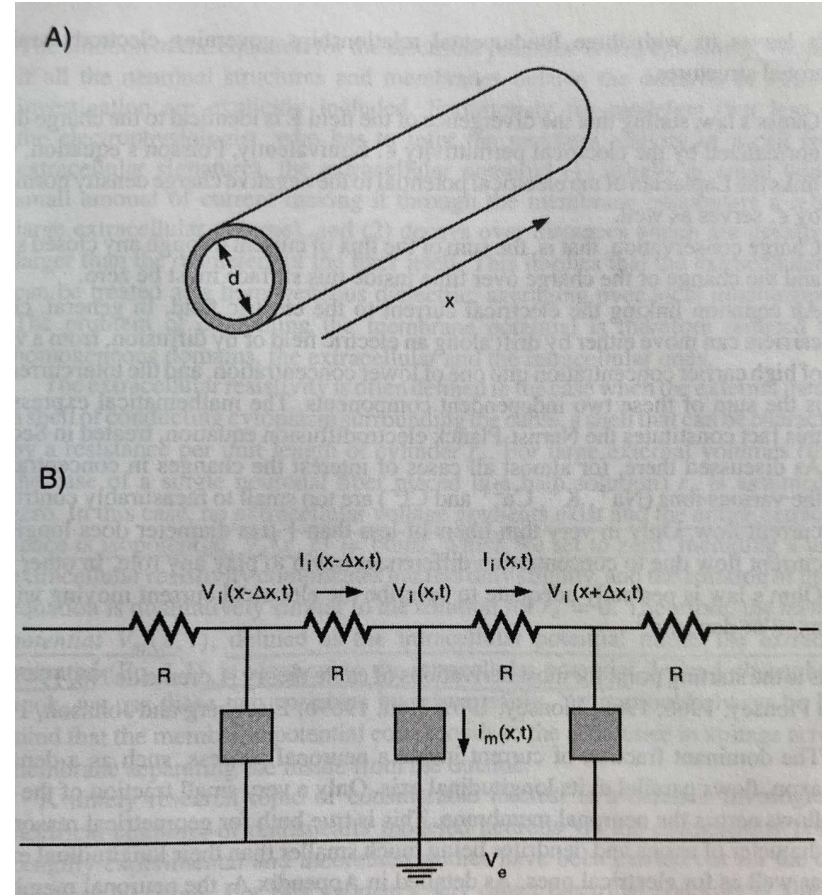
FIG. 1. Diagram illustrating the flow of electric current from a microelectrode whose tip penetrates the cell body (soma) of a neuron. The full extent of the dendrites is not shown. The external electrode to which the current flows is at a distance far beyond the limits of this diagram.



Wilfred Rall (1922-2018)

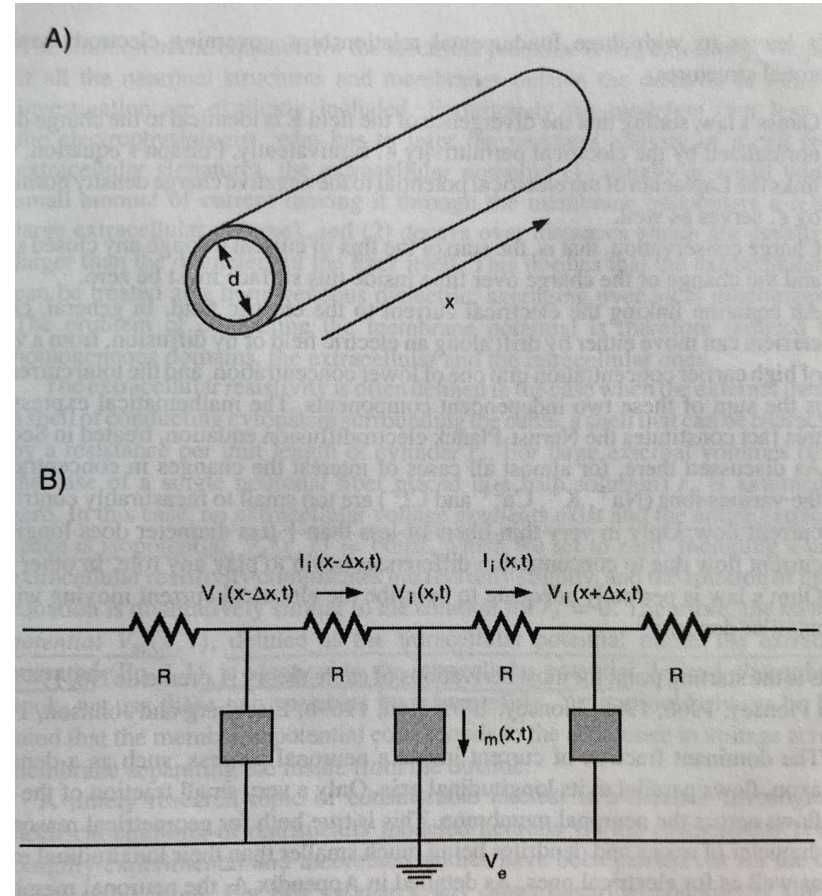
Cable Equation

- Dendrite can be considered a cable of diameter d and length x
- The cable can be split into segments of length Δx
- Each segment can be modelled as an equivalent circuit
- i intracellular, e extracellular, m membrane (i.e. across the membrane)



Cable Equation

- We assume that $V_e(x,t)$ is constant and we can set it to zero
- We assume that E_m or V_{rest} is constant. It can be set to zero. V represents $V_m - V_{rest}$



Cable Equation

Let's consider one cable segment

$$V_i(x, t) - V_i(x + \Delta x, t) = RI_i(x, t)$$

With $\Delta x \rightarrow 0$ and $V_m = V_i$

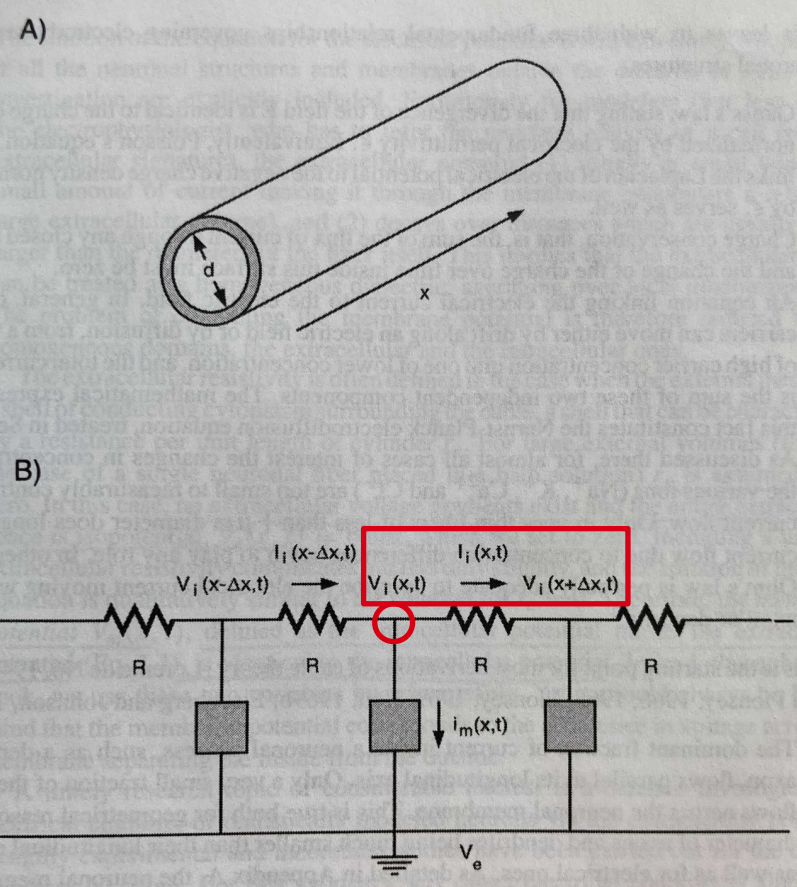
$$\frac{\partial V_m}{\partial x}(x, t) = -r_a \cdot I_i(x, t)$$

The net current passing through one node is 0

$$i_m(x, t)\Delta x + I_i(x, t) - I_i(x - \Delta x, t) = 0$$

$$i_m(x, t) = -\frac{\partial I_i}{\partial x}(x, t)$$

$$\frac{1}{r_a} \frac{\partial^2 V_m}{\partial x^2}(x, t) = i_m(x, t)$$



Cable Equation

Consider a passive cable

$$i_m(x, t) = \frac{V_m(x, t) - V_{\text{rest}}}{r_m} + c_m \frac{\partial V_m(x, t)}{\partial t} - I_{\text{inj}}(x, t)$$

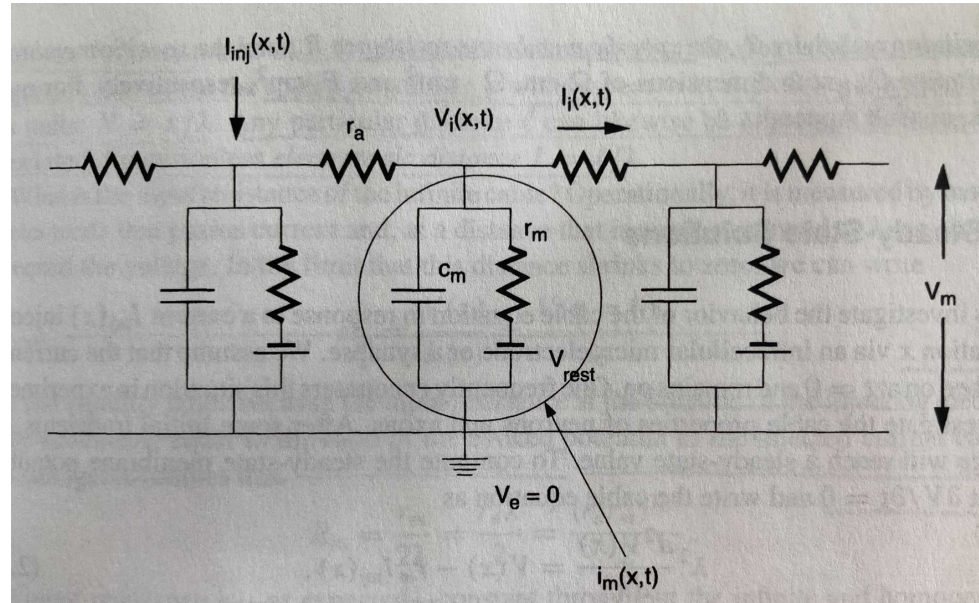
With

Membrane time constant: $\tau = r_m c_m$

Steady-state space constant: $\lambda = \sqrt{r_m / r_a}$

Linear cable equation:

$$\lambda^2 \frac{\partial^2 V_m(x, t)}{\partial x^2} = \tau_m \frac{\partial V_m(x, t)}{\partial t} + (V_m(x, t) - V_{\text{rest}}) - r_m I_{\text{inj}}(x, t)$$



Space and time constants

$$\lambda = \sqrt{r_m / r_a}$$

Steady-state space constant or simply space constant tells us how far a given input propagates along the length of the cable. Space constant is high is the internal medium that does not oppose much resistance and the “cable” is well isolated.

$$\tau = r_m C_m$$

Membrane time constant tell us how much time is needed to charge and discharge the membrane. This time is high is there is a high resistance through the membrane and if we need much time to charge the “capacitor”

Cable Equation

$$\lambda^2 \frac{\partial^2 V_m(x, t)}{\partial x^2} = \tau_m \frac{\partial V_m(x, t)}{\partial t} + (V_m(x, t) - V_{\text{rest}}) - r_m I_{\text{inj}}(x, t)$$

- We assume that E_m or V_{rest} is constant and can be set to zero for simplicity. $V = V_m - V_{\text{rest}}$
- Without injected current, the cable equation takes the compact form:

$$\lambda^2 \frac{\partial^2 V}{\partial x^2} = \tau \frac{\partial V}{\partial t} + V$$

Steady-state solutions of the cable equation

$$\lambda^2 \frac{\partial^2 V_m(x, t)}{\partial x^2} = \tau_m \frac{\partial V_m(x, t)}{\partial t} + (V_m(x, t) - V_{\text{rest}}) - r_m I_{\text{inj}}(x, t)$$

- We inject a current I_{inj} in the position $x=0$ at the time $t=0$ and it remains on
- The voltage changes in time until it arrives to a steady-state. At this point, we can set the derivative of V over time to zero

$$\lambda^2 \frac{d^2 V(x)}{dx^2} = V(x) - r_m I_{\text{inj}}(x)$$

- One end ($x=0$) of the cable is clamped at V_0
- We can solve the equations for several conditions at the other end

Cable Equation

Dimensionless Equation:

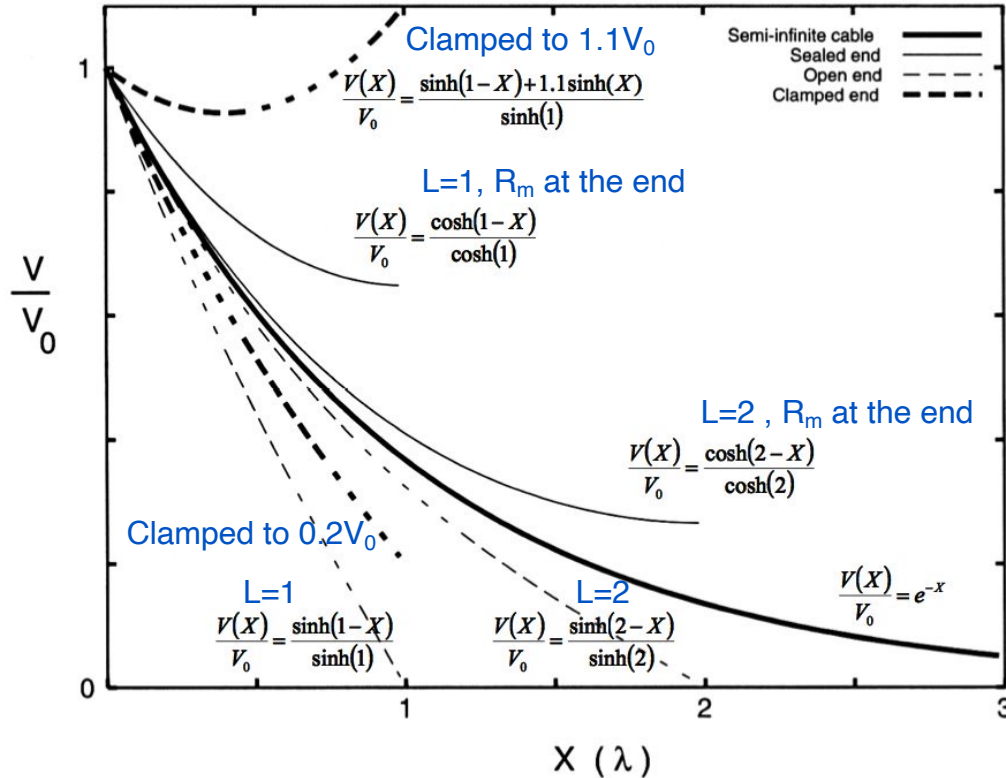
$$\lambda^2 \frac{\partial^2 V}{\partial x^2} = \tau \frac{\partial V}{\partial t} + V$$

$$X = \frac{x}{\lambda}$$

$$T = \frac{t}{\tau}$$

$$\frac{\partial^2 V}{\partial X^2} = \frac{\partial V}{\partial T} + V$$

Steady-state solutions:



Cable Equation Units

$$r_a = \frac{R_i}{Area} = \frac{4R_i}{\pi d^2}$$

$$R_A = lr_a$$

$$G_m = 1/R_m$$

$$r_m = \frac{R_m}{\pi d}$$

$$R_M = r_m/l$$

$$c_m = C_m \pi d$$

$$C_M = C_m l$$

R_A total axial resistance (Ω)

R_M total membrane resistance (Ω)

C_M total membrane capacitance (F)

r_a axial resistance per unit length (Ω/cm)

r_m membrane resistance per unit length ($\Omega \cdot cm$)

c_m membrane capacitance per unit length (F/cm)

R_i intracellular resistivity ($\Omega \cdot cm$)

R_m passive membrane resistivity ($\Omega \cdot m^2$)

G_m leak conductance (S/cm^2)

C_m specific membrane capacitance (F/cm^2)

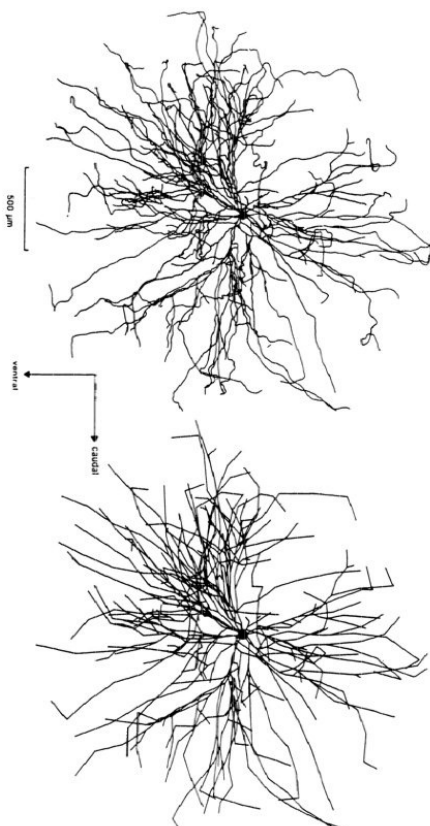
τ_m membrane time constant (sec)

λ membrane space constant (cm)

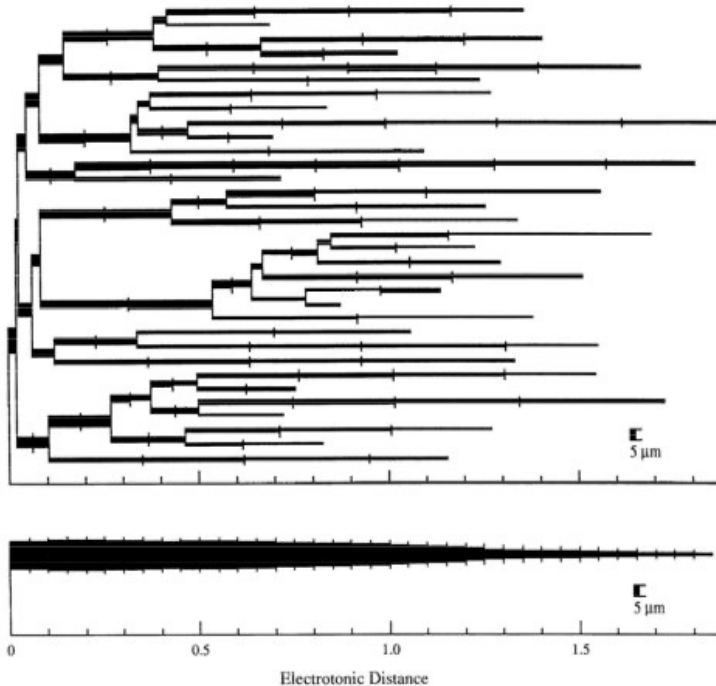
Equivalent cable models

- It is possible to solve the cable equation for time, at the branching points...
- Researchers spent efforts to find solutions of the cable equations for neurons more and more complex
- Rall (1962, 1964) found that under certain conditions, it is possible to reduce a complex morphology into a simple equivalent circuit which can be more easily solved.

Equivalent Cable Models



3/2 Power Law: $d_{parent}^{3/2} = \sum d_{daughter}^{3/2}$
Terminations all occur at same electrotonic distance



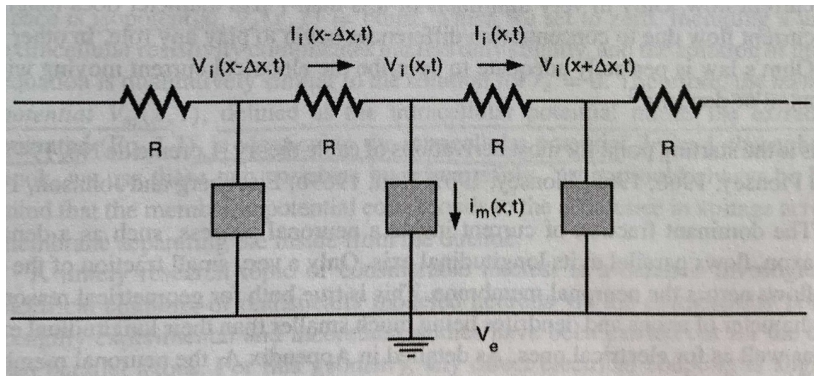
Rall, 1962

Rall W et al. (1992) Matching Dendritic Neuron Models to Experimental Data. *Physiol Rev* 72(4):S159-S186.

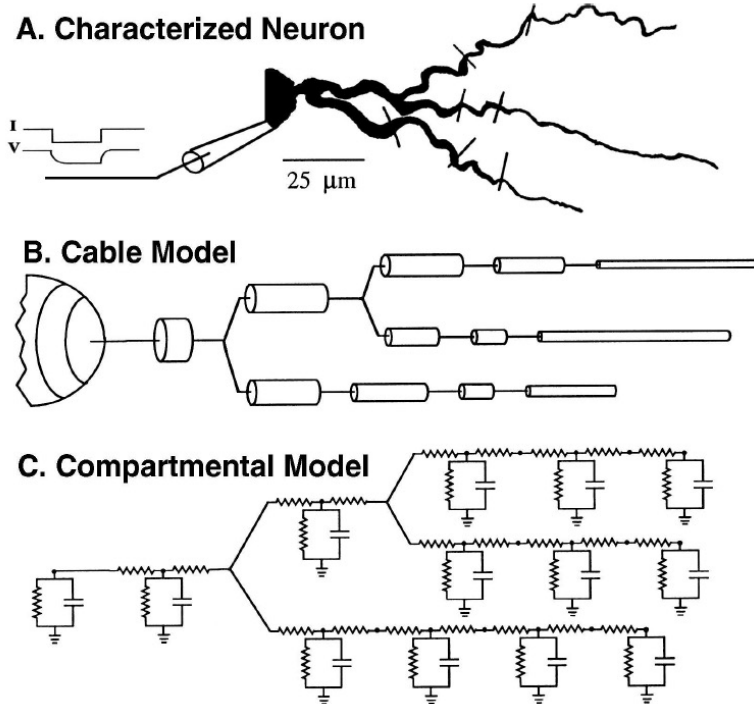
Compartmental modelling

- Exact methods are not scalable
- Neurons have complex shape, receive many (synaptic) inputs, and are highly non-linear
- Non steady-state cable solutions are difficult
- Necessary assumptions may not hold true
- With the advent of computers, the best approach is to use numerical methods
- Dendrites are divided into compartments, small patches of neuronal membranes that are isopotentials
- Compartments are then coupled with other methods (see lecture 13)

Compartmental modelling



i_m can be replaced with the set of active currents, such as the ones seen in HH model



Summary 2

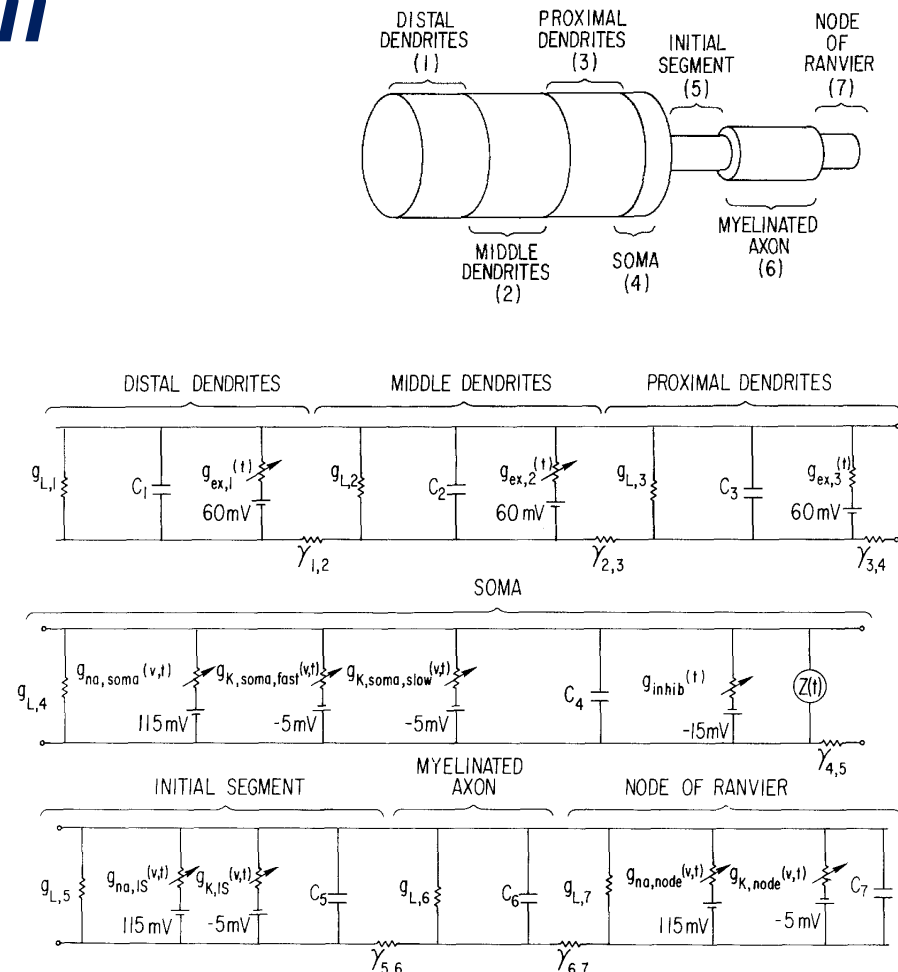
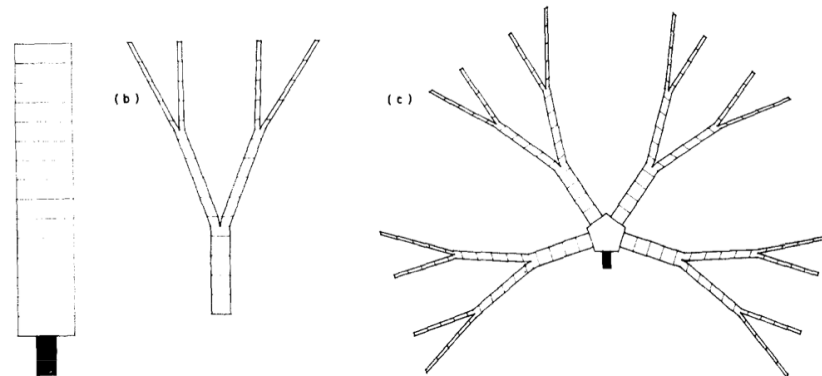
- The complex geometry of the circuit can be divided in discrete compartments and each of them can be represented as an equivalent circuit
- The formalism is similar to the one used in HH model
- The cable equation is a good model for the spatio-temporal behavior of neurons

Lecture Overview

- Scope
- Approaches
- **Applications**

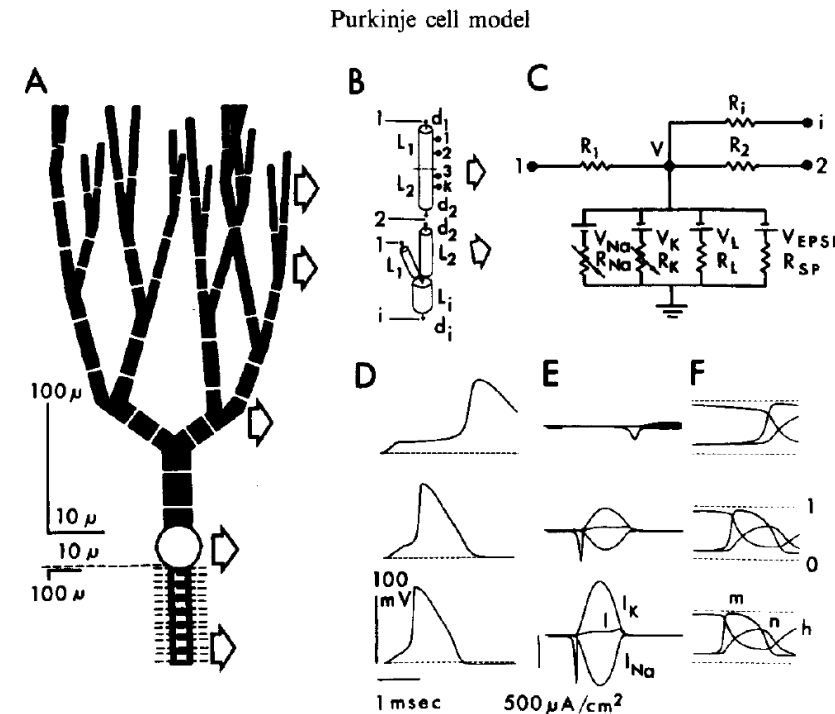
Traub, 1977; Traub and Llinas, 1977

- Spinal cord motoneuron
- HH equations and cable equation
- 2/3 power law (Traub and Llinas, 1977)
- Two-step Euler method (lecture 13)
- IBM 370 Model 168 computer



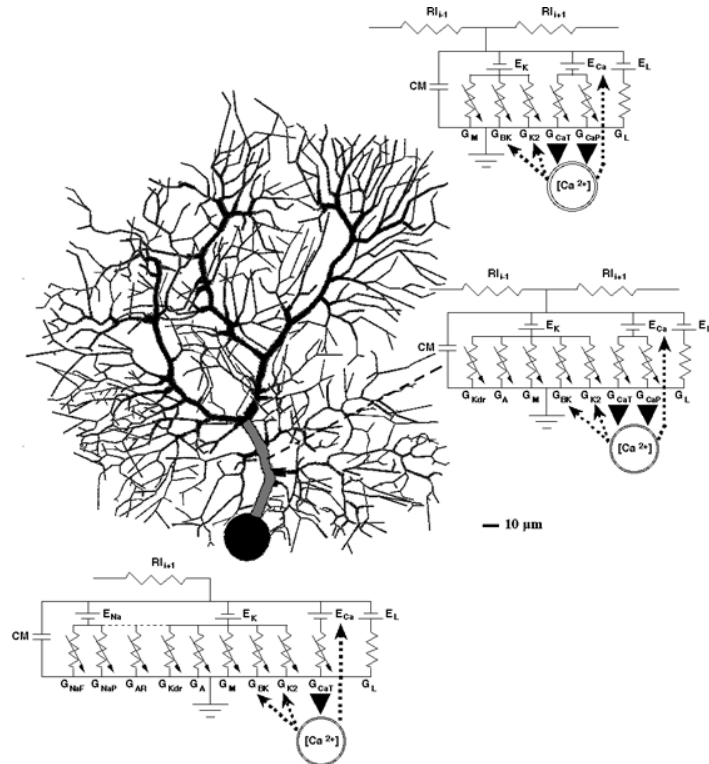
Pellionisz and Llinas, 1977

- Frog Purkinje cell
- Morphological reconstruction from Golgi staining
- 62 spatial compartments
- The active and passive properties are specified independently for each compartment
- 2/3 power law does not apply
- Euler integration
- PDP15 computer



De Schutter and Bower, 1994

- 10 channel types
- 1600 compartments
- channels differentially distributed over three zones (soma, main dendrite, entire dendrite)
- hand-tuned conductances
- two types of spiking behavior



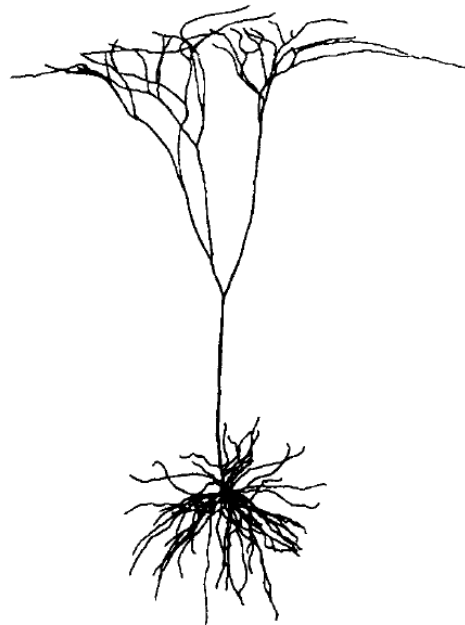
Mainen et Sejnowski, 1996

Influence of dendritic structure on firing pattern in model neocortical neurons

Zachary F. Mainen* & Terrence J. Sejnowski

Howard Hughes Medical Institute, Computational Neurobiology Laboratory,
Salk Institute for Biological Studies, La Jolla, California 92037, and
Department of Biology, University of California, San Diego, La Jolla,
California 92093, USA

NEOCORTICAL neurons display a wide range of dendritic morphologies, ranging from compact arborizations to highly elaborate branching patterns¹. *In vitro* electrical recordings from these neurons have revealed a correspondingly diverse range of intrinsic firing patterns, including non-adapting, adapting and bursting types^{2,3}. This heterogeneity of electrical responsivity has generally been attributed to variability in the types and densities of ionic channels. We show here, using compartmental models of reconstructed cortical neurons, that an entire spectrum of firing patterns can be reproduced in a set of neurons that share a common distribution of ion channels and differ only in their dendritic geometry. The essential behaviour of the model depends on partial electrical coupling of fast active conductances localized to the soma and axon and slow active currents located throughout the dendrites, and can be reproduced in a two-compartment model. The results suggest a causal relationship for the observed correlations between dendritic structure and firing properties³⁻⁷ and emphasize the importance of active dendritic conductances in neuronal function⁸⁻¹⁰.

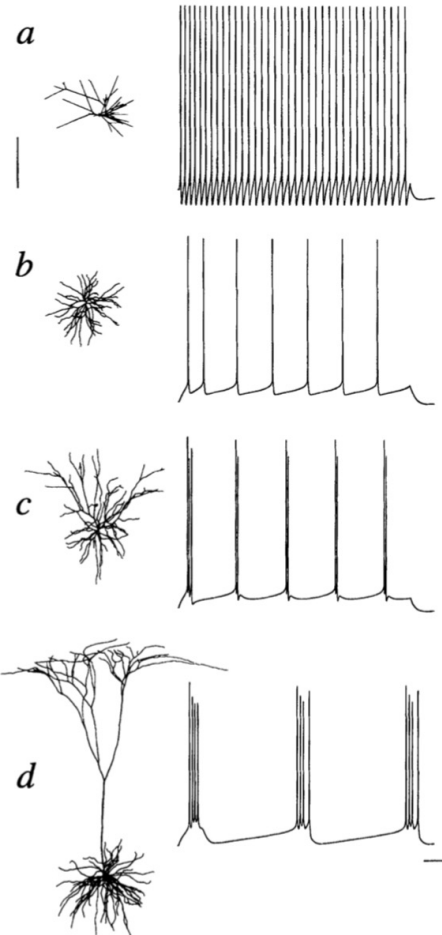


NATURE · VOL 382 · 25 JULY 1996

Mainen et Sejnowski, 1996

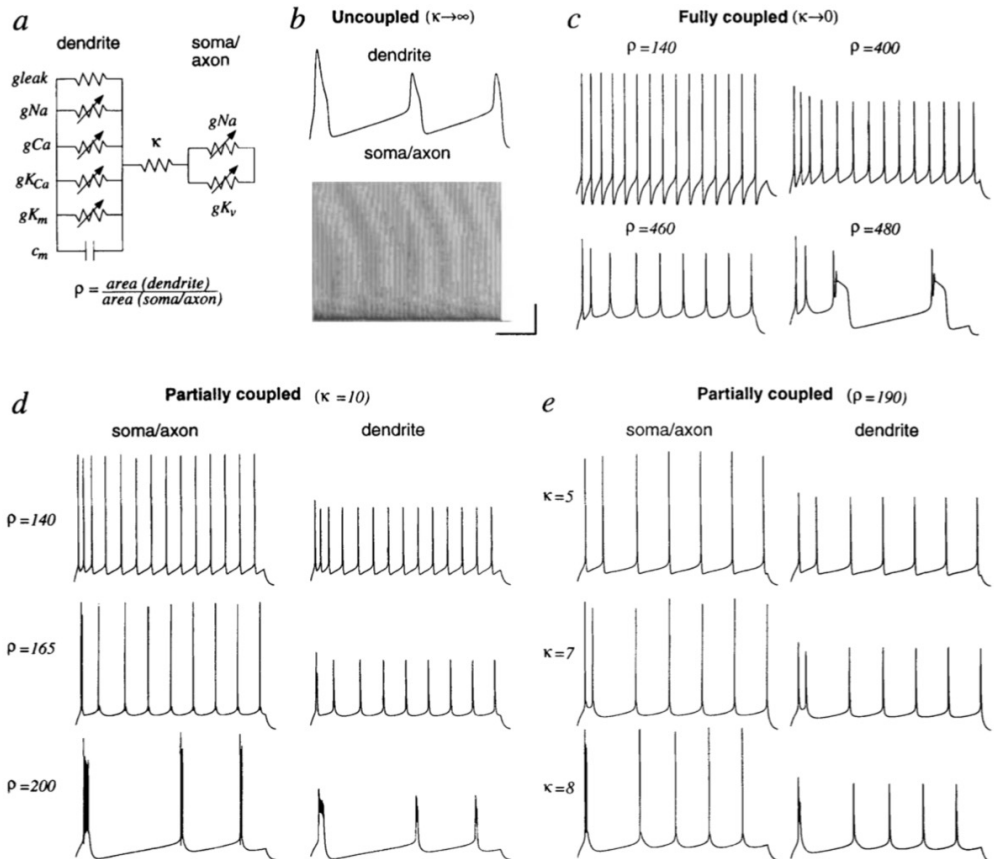
FIG. 1 Distinct firing patterns in model neurons with identical channel distributions but different dendritic morphology. Digital reconstructions of dendritic arborizations of neurons from rat somatosensory cortex (a) and cat visual cortex (b–d). a, Layer 3 aspiny stellate. b, Layer 4 spiny stellate. c, Layer 3 pyramid. d, Layer 5 pyramid. Somatic current injection (50, 70, 100, 200 pA for a–d, respectively) evoked characteristic firing patterns. a shows only the branch lengths and connectivity whereas b–d show a two-dimensional projection of the three-dimensional reconstruction. Scale bars: 250 μ m (anatomy), 100 ms, 25 mV.

All currents were calculated using conventional Hodgkin–Huxley-style kinetics with an integration time step of 250 μ s. Current (I) from each channel type was given by $I = g a^x b (v - E)$, where g is the local conductance density, a is an activation variable with x order kinetics, b is an optional inactivation variable, v is the local membrane potential, and E is the reversal potential for the ionic species ($E_{\text{leak}} = -70$ mV, $E_{\text{K}} = -90$ mV, $E_{\text{Na}} = 50$ mV, $E_{\text{Ca}} = 140$ mV).



Mainen et Sejnowski, 1996

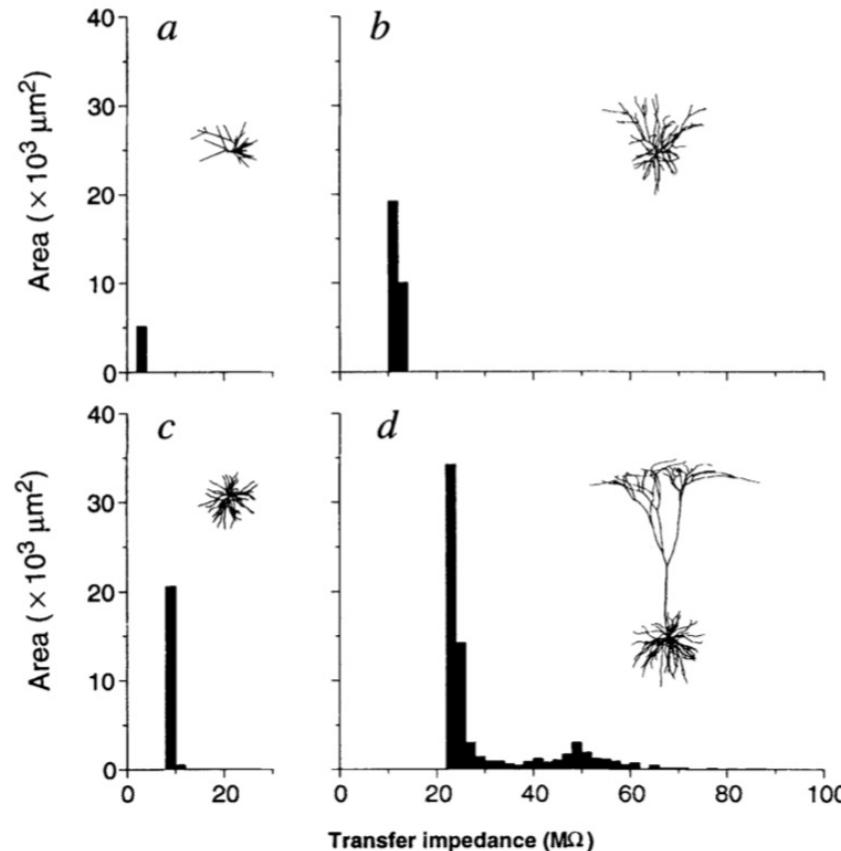
FIG. 2 Effects of electrical structure on firing pattern in a reduced model. *a*, A two-compartment model incorporating the same channels modelled in Fig. 1. The two compartments correspond to the dendritic tree ('dendrite') and the soma and axon initial segment ('axon–soma'). The parameter κ specifies the electrical resistance (coupling) between the two compartments. The parameter ρ specifies the ratio of dendritic to axo–somatic area and thereby sets the strength of dendritic currents relative to axo–somatic currents. The channels and membrane properties of each compartment are depicted.



Mainen et Sejnowski, 1996

FIG. 4 Electrical geometry of cortical cells. Histograms show the distribution of electrical attenuation between the soma and dendritic segments for the four neurons depicted in Fig. 1. The steady-state transfer impedance (Z) from the soma to each simulated dendritic compartment was calculated by injecting a small current step (I) in the soma and measuring the resulting (passive) steady-state voltage change (V) in the dendritic compartment ($Z = V/I$). The histogram bin corresponding to this impedance level was then incremented by an amount equal to the membrane area of that compartment. The total area of the histogram therefore reflects the total dendritic area and the shape of the histogram reflects the relative electrical distance of the dendritic membrane from the soma. These can be compared to the parameters ρ and κ in the reduced model, respectively.

Neuron in d has a big dendritic area (big ρ) and a strong attenuation (small k). Both full and reduced models show bursting behavior. Same reasoning can be applied to the other cases.



Mainen et Sejnowski, 1996

- Previously, it was believed that the diversity of observed somatic firing patterns were mostly due to variability in the types and the densities of ion channels
- Mainen et Sejnowski showed that an entire spectrum of firing patterns can result from different dendritic geometry
- Essential behavior depends on partial electrical coupling of fast conductances in the soma/AIS and slow active currents in the dendrites



Principles Governing the Operation of Synaptic Inhibition in Dendrites

Albert Gidon¹ and Idan Segev^{1,2,3,*}

¹Department of Neurobiology, Alexander Silberman Institute of Life Sciences

²Interdisciplinary Center for Neural Computation

³The Edmond and Lily Safra Center for Brain Sciences

The Hebrew University of Jerusalem, Jerusalem 91904, Israel

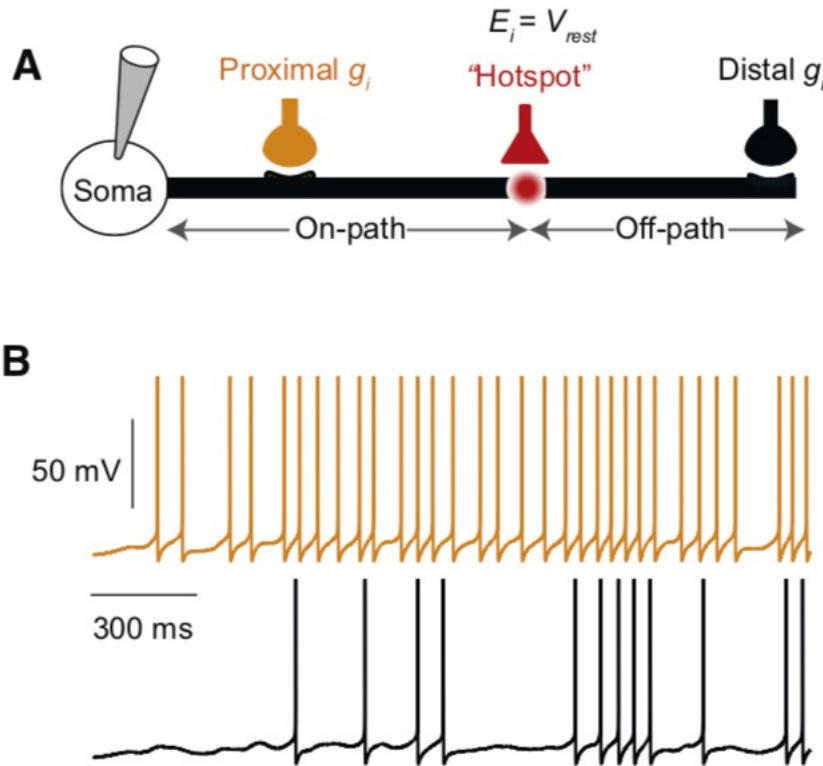
*Correspondence: idan@lobster.ls.huji.ac.il

<http://dx.doi.org/10.1016/j.neuron.2012.05.015>

SUMMARY

Synaptic inhibition plays a key role in shaping the dynamics of neuronal networks and selecting cell assemblies. Typically, an inhibitory axon contacts a particular dendritic subdomain of its target neuron, where it often makes 10–20 synapses, sometimes on very distal branches. The functional implications of such a connectivity pattern are not well understood. Our experimentally based theoretical study highlights several new and counterintuitive principles for dendritic inhibition. We show that distal “off-path” rather than proximal “on-path” inhibition effectively dampens proximal excitable dendritic “hotspots,” thus powerfully controlling the neuron’s output. Additionally, with multiple synaptic contacts, inhibition operates globally, spreading centripetally hundreds of micrometers from the inhibitory synapses. Consequently, inhibition in regions lacking inhibitory synapses may exceed that at the synaptic sites themselves. These results offer new insights into the synergistic effect of dendritic inhibition in controlling dendritic excitability and plasticity and in dynamically molding functional dendritic subdomains and their output.

Gidon et Segev, 2012



(A) A model of a cylindrical cable (sealed end at $L = 1$) coupled to an iso-potential excitable soma. Twenty NMDA synapses are clustered at the hotspot located at $X = 0.6$; each synapse is randomly activated at 20 Hz. A single inhibitory synapse ($g_i = 1$ nS) is placed either distally or proximally at the same electrotonic distance ($X = 0.4$) from the hotspot.

(B) Inhibition of the somatic Na^+ spikes is more effective when inhibition is placed distally to the hotspot (black synapse and corresponding black somatic spikes, compared to orange synapse and corresponding orange somatic spikes).

Figure 1. Off-Path Inhibition Is More Effective than the Corresponding On-Path Inhibition in Dampening a Local Dendritic Hotspot

Gidon et Segev, 2012

- The paper derives a counterintuitive principle for dendritic inhibition, namely that “off-path” inhibition can more effectively dampen proximal excitable “hotspots” than “on-path” inhibition
- Highlights that inhibition spreads far beyond the actual location of the inhibitory synapse, giving a new perspective on the “global” reach of inhibitory connections that are often mediated by 10-20 synapses/connection
- The asymmetry of the impact of distal versus proximal inhibition on location h (the hotspot) results from the difference in the model’s boundary conditions, namely, sealed-end boundary at the distal end and an isopotential soma at the proximal end.

Summary 3

- The history of modeling the cable properties of neurons is also a history of computational capability; early models used symmetries to simplify computation and with more available compute power, more detailed model could be built
- Those detailed models extend the theoretical insights from early studies of the cable equation applied to neuronal modeling to more specific and experimentally-based theoretical insights (e.g. how specific dendrites shape somatic firing)
- Importantly, even today, many decades after the seminal work of Rall, there are still fundamental theoretical insights to be made into the cable-equation formulation of neurons

Lecture Summary

- Neurons are electrically active cells, this electrophysiological behavior manifests in different forms (e.g. somatic firing, dendritic integration, extracellular field)
- Depending on what aspects are studied, different formalisms for describing a neuron's electrophysiology are available ranging from a biochemical reaction-diffusion formalism, to a biophysical cable representation to abstract point neurons
- The cable representation combined with ion channel representations is an important formalism allowing deep insights into a neuron's input output function and its role as a biophysical building block in the brain
- These biophysically detailed models provide a strong link to experiment as their variables relate to directly measurable observables

What you have learn

- HH model. Understand the principles. Remember the fundamental equations and definition. It is not necessary to remember the equations for the rate constants.
- Cable equation. Understand the principles. Remember the schema. Remember the fundamental equations and definition. It is not necessary to remember the analytical solutions.
- Units.
- 3/2 power law.
- Compartmental model.
- You do not have to remember the details of the papers cited in the section “applications”. However, try to retain the main points.

References

- Bertil Hille – Ion Channels of Excitable Membranes – Third edition
- Christof Koch – Biophysics of Computation